

# Ultrahigh Performance of Nanoengineered Graphene-Based Natural Jute Fiber Composites

Forkan Sarker,<sup>†,‡</sup> Prasad Potluri,<sup>\*,†,‡</sup> Shaila Afroj,<sup>§,||</sup> Vivek Koncherry,<sup>†,‡</sup> Kostya S. Novoselov,<sup>§,||</sup> and Nazmul Karim<sup>\*,||</sup>

<sup>†</sup>School of Materials, The University of Manchester, Oxford Road, Manchester, M13 9PL, U.K.

<sup>‡</sup>Northwest Composites Centre, The University of Manchester, Oxford Road, Manchester, M13 9PL, U.K.

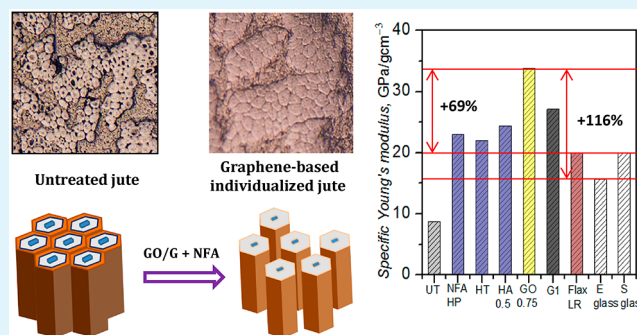
<sup>§</sup>School of Physics & Astronomy, The University of Manchester, Oxford Road, Manchester, M13 9PL, U.K.

<sup>||</sup>National Graphene Institute (NGI), The University of Manchester, Booth Street East, Manchester, M13 9PL, U.K.

## Supporting Information

**ABSTRACT:** Natural fibers composites are considered as a sustainable alternative to synthetic composites due to their environmental and economic benefits. However, they suffer from poor mechanical and interfacial properties due to a random fiber orientation and weak fiber–matrix interface. Here we report nanoengineered graphene-based natural jute fiber preforms with a new fiber architecture (NFA) which significantly improves their mechanical properties and performances. Our graphene-based NFA of jute fiber preform enhances the Young modulus of jute–epoxy composites by ~324% and tensile strength by ~110% more than untreated jute fiber composites, by arranging fibers in a parallel direction through individualization and nanosurface engineering with graphene derivatives. This could potentially lead to manufacturing of high-performance natural alternatives to synthetic composites in various stiffness-driven applications.

**KEYWORDS:** graphene, graphene oxide, jute fibers, natural fiber composites, mechanical properties



Natural fiber reinforced composites (FRC) have been the focus of much attention over recent years due to their potential to replace environmentally unfriendly synthetic FRC.<sup>1</sup> Moreover, natural fibers come from the renewable resource and can easily be recycled or burned with less residue and CO<sub>2</sub> emission to the atmosphere.<sup>1,2</sup> Such lightweight and environmentally sustainable natural FRC could ideally be used as a replacement of glass, carbon, or other synthetic FRC,<sup>3</sup> in numerous applications such as automotive, construction and household.<sup>4</sup> Jute, flax, hemp, and sisal are the main dominating bast fibers that are used as reinforcing materials for natural FRC. Among them, jute fibers have been a popular choice as reinforcing materials for composites due to lower production cost, lower density, long individual fiber length, and better mechanical properties than other natural alternatives.<sup>5</sup> However, jute FRC still suffer from poor mechanical properties, when compared with synthetic fibers (such as glass).<sup>6</sup>

The mechanical properties of FRC are mainly dominated by (a) the properties of reinforcing materials which are considered to be the main load bearing constituents and (b) the interface between the fiber and matrix which transfer the load from the matrix to reinforcing materials through shear stress.<sup>7,8</sup> Alkali treatment is a popular technique to enhance the

mechanical properties of natural FRC by improving the load bearing capacity of reinforcing materials and creating a strong fiber–matrix interface.<sup>9,10</sup> It removes impurities such as wax, hemicellulose, and lignin from the fiber surface and separates elementary fibers from technical fibers in order to improve the fiber packing in composites. As suggested in previous studies,<sup>6,11–13</sup> the treatment with a lower alkali concentration (~0.5 wt %) for a prolonged time is an effective technique to enhance the mechanical properties of jute fiber. However, there are still flaws<sup>5</sup> (microvoids) present in the fiber even after the alkali treatment that inhibits fibrils to carry more loads and produce a weak fiber/matrix interface. There have been many efforts to enhance the performance of composites by removing these flaws either through nanomaterial grafting<sup>7,14–18</sup> or surface modifications such as silane treatment,<sup>19</sup> acetylations,<sup>20</sup> etherification,<sup>21</sup> and peroxide<sup>22</sup> and plasma treatment.<sup>23</sup> However, such treatments are expensive and time-consuming process with very limited improvement in composites performances.

Received: March 15, 2019

Accepted: May 7, 2019

Published: May 7, 2019

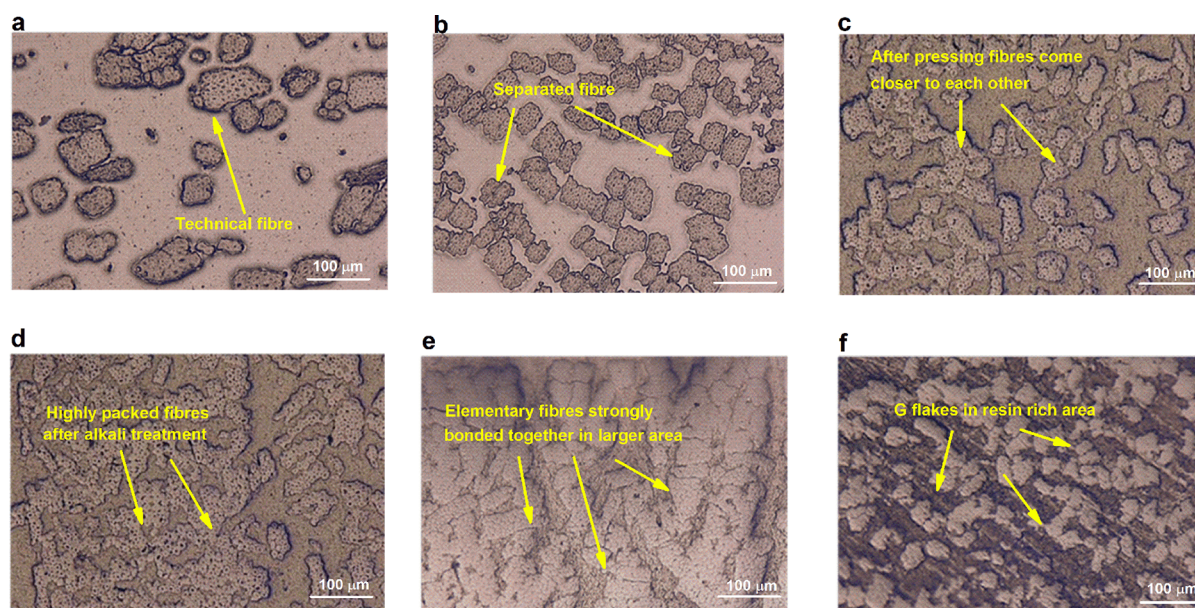


**Figure 1.** Optical microscopic cross-sectional image of jute fiber epoxy composites: (a) untreated fiber composites, UT ( $\times 500$ ); (b) fibrillated jute fiber composites with NFA ( $\times 500$ ); (c) NFA composites with pressing, NFAHP ( $\times 500$ ); (d) alkali treated composites HA0.5 ( $\times 500$ ); (e) GO coated composites GO 0.75 ( $\times 500$ ); and (f) G flake coated composites G10 ( $\times 500$ ).

Graphene-based materials have shown huge potential for composite applications due to their excellent mechanical properties. Graphene oxide (GO) is a graphene derivative, which is formed by attaching various oxygen functional groups (e.g., hydroxyl, epoxy, and carbonyl groups) to their basal plane and edges of a graphene sheet.<sup>15,24,25</sup> Therefore, GO could add functionality to fibers and enhance the strength and toughness at the fiber/matrix interface.<sup>26</sup> Several studies reported the use of GO to improve the performance of synthetic composites such as grafting of GO onto glass fibers<sup>7</sup> and carbon fabric,<sup>18</sup> and blending of GO into epoxy resin for carbon/epoxy composites.<sup>27</sup> Moreover, graphene nanoplatelets (GNP) or graphene flakes (G) have been investigated for composite applications,<sup>28–32</sup> as such materials could be produced in large quantity.<sup>33</sup> The study suggested that GNP could prevent the delamination of the fibers<sup>31</sup> and can delay the crack propagation at the interphase by redistributing the stress around fibers, where the cracks started to form.<sup>18</sup> However, very limited study has been carried out on natural fiber-based composites for structural applications. In our previous study, we report that the coating of graphene materials (GO and G flakes) onto jute fibers enhanced interfacial shear strength and tensile strength of individual fibers by  $\sim 236\%$  and  $\sim 96\%$ , respectively.<sup>6</sup> However, the main challenge is how we could translate such excellent properties achieved on individual fibers to a jute fiber reinforced composite for real world applications.

Here we address this challenge by reporting a novel strategy to manufacture the next generation of natural fiber reinforced composites by combining physical and chemical modification of jute fibers preforms. A simple hand combing was used to individualize jute fibers with subsequent alkali treatment to remove noncellulosic impurities from the jute fiber surface. Then jute fiber was modified by GO and G flakes with subsequent hot pressing to produce preforms with a new fiber architecture (NFA); before jute/epoxy composites were made by a vacuum resin infusion process. The improvement in longitudinal and transverse mechanical properties of compo-

sites with surface treatment and NFA of jute fiber preforms was tested using a tensile tester. The fracture surface of tested specimen was analyzed using a scanning electron microscope (SEM). Finally, obtained tensile and specific properties of as prepared jute fibers composites were compared with that of glass and flax fibers and also with results reported in the literatures for surface-modified natural fibers.

## RESULTS AND DISCUSSION

**Improved Fiber Volume Fraction with Physical and Chemical Treatments.** The fiber volume fraction ( $V_f$ ) of FRC has a significant effect on mechanical properties (such as strength, stiffness, and toughness) of the composites materials.<sup>34</sup> The strength and stiffness of a composite laminate increases proportionally with the increase of  $V_f$  up to  $\sim 80\%$ , at which the amount of resin is sufficient to hold the fibers properly.<sup>35</sup> However, jute fiber composites suffer from relatively lower  $V_f$  ( $\sim 23\%$ ) during the vacuum infusion process like other natural fiber composites and may be due to the presence of impurities and interfibrillar arrangement in the fiber. Moreover, the presence of waxes, lignin, and hemicellulose in jute fibers provides a very smooth fiber surface (Figure S2a, Supporting Information) and do not allow fibrils to come out and pack inside the composites, Figure 1a. Therefore, a lower  $V_f$  value is obtained, which usually results in jute fiber reinforced composites with a poor failure mode and ultimate strength.<sup>36</sup>

In order to improve the mechanical properties of jute FRC, here we developed jute fiber preforms with novel surface treatments and a new fiber architecture (NFA) that would increase  $V_f$  significantly by exposing jute fibers to physical (combing and hot pressing) and chemical treatments (alkali and graphene-based materials). We perceived the increment of  $V_f$  after each treatment by observing the cross-section of jute/epoxy composites under an optical microscope, Figure 1a–f. The combing of jute fibers increases  $V_f$  by  $\sim 10\%$  to  $\sim 33\%$  due to the increase in the degree of fiber separation in the preform<sup>37</sup> and fiber packing in the composites as shown in

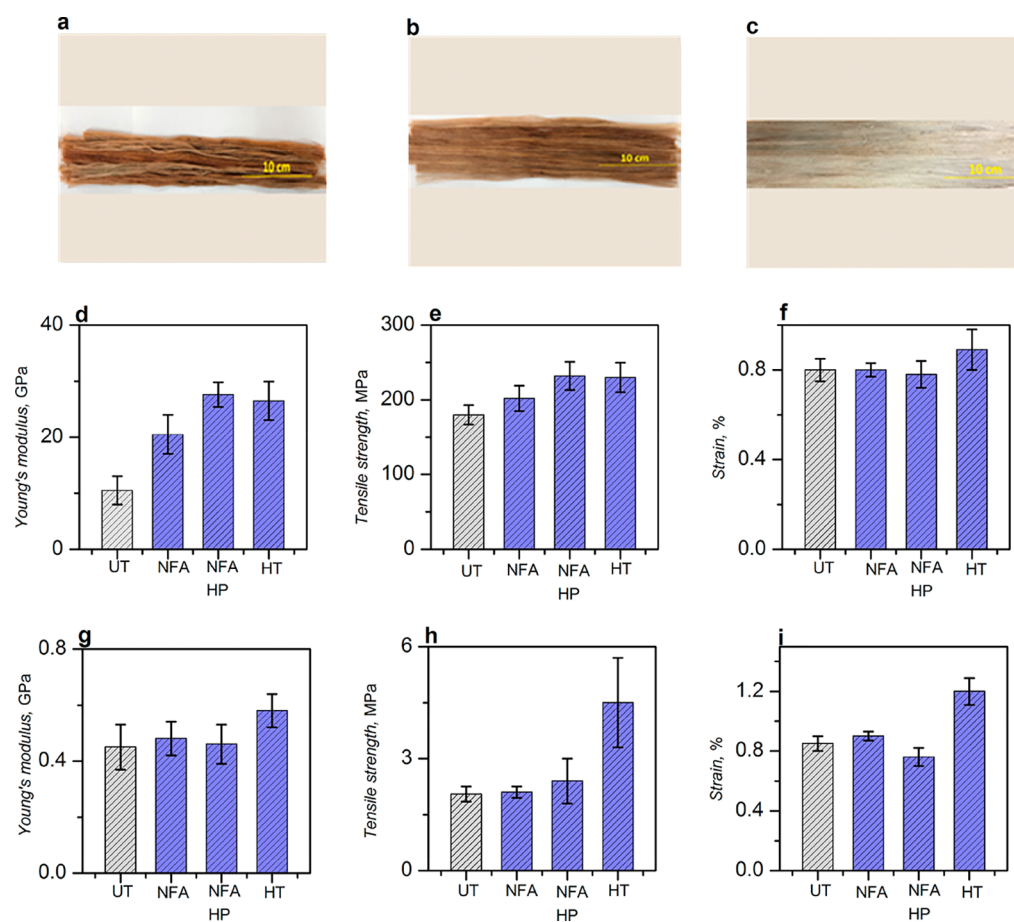


**Figure 2.** (a) Untreated fiber, UT preform; (b) fibrillated fiber preform, NFA; (c) fibrillated and compacted preform, NFAHP; (d) longitudinal Young's modulus of untreated and fibrillated jute fiber composites; (e) longitudinal tensile strength of untreated and fibrillated jute fiber composites; (f) longitudinal tensile strain% of untreated and fibrillated jute fiber composites; (g) transverse Young's modulus of untreated and fibrillated jute fiber composites; (h) transverse tensile strength of untreated and fibrillated jute fiber composites; (i) transverse tensile strain % of untreated and fibrillated jute fiber composites.

Figure 1b. We then applied hot pressing on the combed fiber in order to achieve a NFA that results in a significant increase of  $V_f$  to  $\sim 47.5\%$ , which is in agreement with previous studies.<sup>38–40</sup> They reported a  $V_f$  of  $\sim 60\text{--}70\%$  with unidirectional natural fiber composites at a constant compaction pressure and  $\sim 35\text{--}40\%$  for composites with randomly oriented fibers. However, all the processes mentioned in the literature are based on liquid molding (i.e., hand lay-up, RTM). In contrast, we report for the first time the manufacturing of a compact dry jute fiber preform (Figure S2b, Supporting Information) with a new architecture in order to improve the fiber packing. Such NFA will enable potential manufacturing of composites with complex structure and excellent drapability.

We then investigated the effects of chemical treatments on  $V_f$  of jute/epoxy composites. The alkali (0.5 wt %) treatment of combed jute fibers and subsequent hot pressing increases  $V_f$  to  $\sim 54\%$ . Alkali treatment removes hemicellulose present between the fibrils and improves the fiber packing within the jute/epoxy composites, Figure 1d. The coating with graphene-materials on combed and alkali treated fibers increases  $V_f$  slightly to  $\sim 55\%$  (with G Flakes) and  $\sim 56\%$  (with GO) after compaction with a hot press. The coating with GO provides slightly better  $V_f$  than that of G flakes coated fibers may be due to strong bonding between oxygen containing functional groups of cellulosic fibers and that of GO, Figure 1e.<sup>6,24,41</sup> In contrast, G-flake coated jute fibers do not produce strong

bonding due to the absence of an oxygen functional group.<sup>28</sup> Moreover, Figure 1f shows agglomeration of G flakes around the fiber surface and matrix.

**Enhanced Mechanical Properties with NFA and Physical Treatments.** Jute fiber contain large amount of (20–50 wt %) of non-cellulosic materials such as hemicellulose and lignin. Such non-cellulosic materials are responsible for the lower crystallinity and hydrophilic nature of jute fibers. Moreover, UT jute fibers contain mostly technical fiber bundles (consists of individual elementary fibers, Figure 2a), which is found to have  $\sim 41\%$  less Young's modulus and  $\sim 39\%$  less tensile strength than the individual elementary fiber (Table S1, Supporting Information). Furthermore, lower  $V_f$  is obtained with UT jute fiber composites. Therefore, jute fiber composites suffer from poor tensile properties when reinforced with epoxy matrix. We obtain a lower Young modulus ( $\sim 10$  GPa) and tensile strength ( $\sim 180$  MPa) with untreated jute/epoxy composites, Figure 2d.

We therefore developed a new fiber architecture (NFA) for the jute fiber preform by using a simple hand combing process, Figure 2b. This results in an increment in individualized and homogeneous elementary fibers with fewer defects and better mechanical properties.<sup>42</sup> The Young's modulus and tensile strength are increased by  $\sim 95\%$  to  $\sim 20.5$  GPa and  $\sim 12\%$  to  $\sim 202$  MPa, respectively, for jute/epoxy composites with NFA (Figure 2d,e and Table S2, Supporting Information) than that

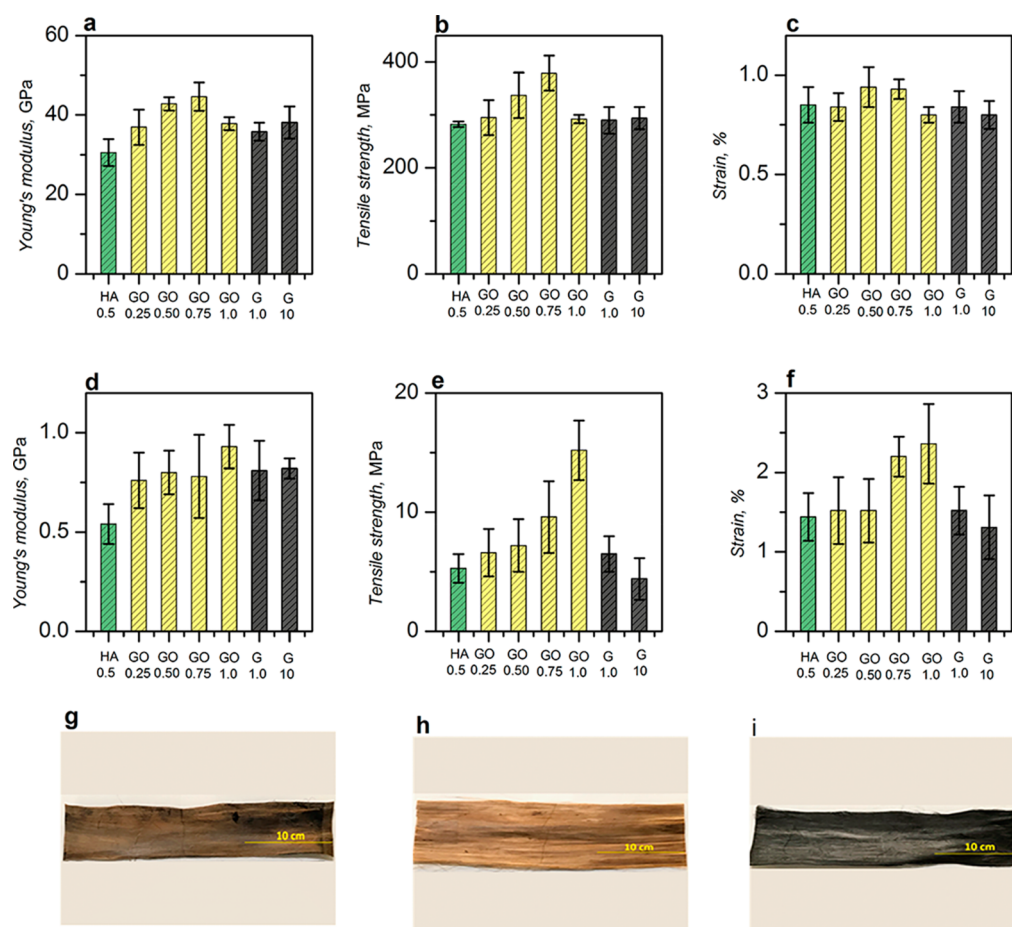


**Figure 3.** (a) Longitudinal Young's modulus of alkali and graphene jute fiber composites; (b) longitudinal tensile strength of alkali and graphene jute fiber composites; (c) longitudinal tensile strain % of alkali and graphene jute fiber composites; (d) transverse Young's modulus of alkali and graphene jute fiber composites; (e) transverse tensile strength of alkali and graphene jute fiber composites; (f) transverse tensile strain % of alkali and graphene jute fiber composites; (g) alkali treated fiber, HA0.5 preform; (h) GO coated preform, GO0.75; and (i) G-flakes coated preform, G1.

of UT composites. Such a significant improvement in the mechanical properties of the composites could be associated with structural mechanics of reinforcing fibers and their increased load bearing capacity. Moreover, NFA composites show higher fiber content ( $V_f$ ) due to the combing process, whereas in UT fiber composites, most of the fiber bundles agglomerated in the cross section, Figure 1a.

We then employ a popular compaction technique with pressing in order to produce NFAWP jute/epoxy composites. Such physical treatment increases fiber packing significantly and also the Young's modulus ( $\sim 27.6$  GPa) and tensile strength ( $\sim 232$  MPa) by  $\sim 34\%$  and  $\sim 15\%$ , respectively, than NFA jute/epoxy composites. The combination of individualization (combing) and compaction (pressing) improves the packing capacity of the composites significantly and increases their load bearing capacity during tensile tests. Further hot water treatment (HT) increases  $V_f$  marginally; however, a slight decrease in the stiffness and strength of the composites is observed and may be due to the change in the biochemical compositions and macromolecular arrangement.<sup>43</sup>

We also carried out the transverse tensile tests of jute/epoxy composites in order to better understand the effect of NFA and physical treatments on the improvement of interfacial shear strength and mechanical properties. A strong bond is needed for better transverse tensile strengths and even for better water resistance of polymer composites.<sup>44</sup> When compared with

longitudinal properties, transverse tensile properties of the composites are found to be lower because of the fiber geometry. Reinforcing fibers are usually distributed parallelly in the direction of loading and hence unable to carry the significant amount of load in the transverse direction as they do in the longitudinal direction. Figure 2g–i show poor transverse properties of the composites with UT jute fibers, due to the presence of impurities (such as fat, waxes, lignin, pectin, and hemicellulose) in the fibers that contribute to the poor adhesion between the fiber and matrix. Even with NFA and physical treatments, no improvement in transverse tensile properties is observed. However, after treatment with hot water (HT), transverse tensile strength of HT fiber composites become more than double ( $\sim 10.6$  MPa) than that of UT fibers ( $\sim 4.16$  MPa). This could be explained by the strong interfacial shear strength of HT fibers with epoxy resin than that of UT fibers.<sup>6</sup> Such behavior of the fibers towards epoxy resin gives a preliminary indication of active fiber surface, either by removing the impurities or filling the flaws, that would bond or cross-link with resin in order to produce a strong interface.

**Ultra-High Performance of Nanoengineered Graphene-Based Composites.** Alkali pretreatment is necessary for jute fibers in order to remove natural impurities and noncellulosic materials. Moreover, the alkali treatment increases the surface roughness by disrupting hydrogen bonding on the fiber surface. Furthermore, the presence of

constituents like hemicellulose can restrict the fiber separation or individualization, as it is connected with the help of lignin matrix. The alkali treatment removes such constituents (lignin and hemicellulose) and improves fiber packing and fiber–matrix adhesion. The removal of hemicelluloses after alkali treatment was confirmed by using the FTIR (Figure S9, Supporting Information). As shown in Figure 3a–c, the Young's modulus increases from  $\sim 27.6$  GPa to  $\sim 32$  GPa and the tensile strength increases from  $\sim 232$  MPa to  $\sim 282$  MPa after 0.5% alkali treatment of the jute fiber preform (Table S2, Supporting Information). Moreover, tensile properties of composites are generally dominated by the fiber properties and fiber orientations.<sup>9</sup> After the mild alkali (HA0.5) treatment, the jute fiber surface becomes very clean (Figure S5b, Supporting Information), due to the removal of alkali sensitive bonds present between fiber components,<sup>9</sup> which contributes to the better stress transfer between the ultimate cells. Furthermore, the better fiber packing and larger amount of parallel fibers allow composites to bear a higher amount of applied load. Thus, the combination of NFA, physical, and heat-alkali treatments (HA0.5) improves the Young's modulus by  $\sim 56\%$  and tensile strength by  $\sim 56.6\%$  than that of UT jute/epoxy composites.

Recent studies have highlighted that the tensile properties of natural fiber can be improved significantly by introducing nanoengineered surface finishes.<sup>7,14,18,45–49</sup> Such studies report that the grafting of nanomaterials on natural fibers surface increases the surface wettability and roughness and therefore improves the mechanical properties. Similarly, here we improve the Young's modulus and tensile strength of the jute/epoxy composite significantly by nanoengineering of the natural fibers surface with graphene materials. The Young modulus, tensile strength, and strain % increase with the increase of GO concentration up to 0.75 mg/mL, Figure 3a–c. At 0.75 mg/mL concentration of GO, we obtain  $\sim 39.3\%$  and  $\sim 34\%$  increments in the Young's modulus ( $\sim 44$  GPa) and tensile strength ( $\sim 379$  MPa), respectively, compared to that of HA0.5 composites. The combination of physical and chemical treatments of the jute–epoxy composites with NFA and nanosurface engineering with GO provides  $\sim 324\%$  improvement in the Young's modulus and  $\sim 110\%$  tensile strength of the composites.

The enhanced mechanical properties of GO-treated jute–epoxy composites could be due to two main reasons: (1) strong adhesion between GO flakes and HA 0.5 treated fiber and (2) interaction of GO-treated jute fiber with the matrix.<sup>6</sup> The oxygen containing functional groups of GO<sup>41</sup> can create a strong bond with HA treated fibers<sup>50</sup> and make them capable of carrying more load from the matrix.<sup>6</sup> The higher magnification cross-section of the image of GO-treated jute–epoxy composites reveals that the elementary fiber, which was separated after the alkali and combing process, are again strongly connected to each other to produce a strong fiber packing inside the composites. Moreover, we do not observe any porosity related issues in the composites, as GO flakes probably fill those porous spaces. Furthermore, GO contains epoxy groups that could lead to a ring-opening reaction and the formation of C–N bonds when exposed to amine groups of the epoxy resin.<sup>11</sup> In addition, a strong hydrogen bond and mechanical interlocking between GO and the epoxy matrix (Figure S5c, Supporting Information) are also possible due to oxygen containing groups and the wrinkle structure of GO, respectively.<sup>51</sup>

We obtain 0.75 mg/mL as the threshold concentration for GO coating on HA0.5 treated jute fibers, as tensile properties deteriorate after this concentration. This may be due to the agglomeration of GO flakes at higher concentration in an epoxy matrix. We then compare the tensile properties of GO treated fiber with G-flakes (G1 and G10) treated jute–epoxy composites. Similar to the single fiber tensile properties,<sup>6</sup> G-flakes do not contribute much to the tensile strength and may be due to the absence of functional groups in their structure; but it increases the Young's modulus of the composites by  $\sim 19\%$  compared to HA0.5 composites, (Figure 3a and Table S2, Supporting Information). The improvement in the Young's modulus of the composites might be due to the uniform deposition of a large amount of G-flakes on the fiber surface and filling of microvoids present in the HA-treated fibers that would help to carry a larger amount of the load (Figure S5d, Supporting Information).

To better understand the effect of nanoengineering with GO on the interfacial shear strength and mechanical properties of jute–epoxy composites; we carried out the transverse tensile testing of composites, Figure 3d–f. The treatment with alkali (HA0.5) increases the transverse tensile strength ( $\sim 5.28$  MPa), which is in agreement with previous studies,<sup>52,53</sup> where they found that alkali treatment improves the transverse tensile strength of natural fiber composites by  $\sim 30$ – $150\%$ . Moreover, alkali treatment improves surface wettability and roughness by removing lignin and hemicelluloses, thus enabling better penetration of resin and improving the fiber–matrix interaction at the composite interfaces. Figure 3d–f shows that the transverse properties of jute–epoxy composites are significantly improved further by GO coating. The transverse tensile strength increases linearly with the increase of GO concentrations, Figure 3e. We achieve maximum transverse tensile strength ( $\sim 15.26$  MPa) with 1 mg/mL GO, which is  $\sim 560\%$  and  $\sim 189\%$  improvement than the untreated and HA0.5 treated jute fiber epoxy composites, respectively. After the alkali treatment, the hydrogen bonding network in the fiber would break and the hydroxyl groups of cellulose become more active to promote hydrophilicity of the fiber as well as compatibility with the GO sheets. Moreover, GO coated fibers contain a significant amount of oxygen containing functional groups such as hydroxyl ( $-\text{OH}$ ), epoxide ( $\text{C}-\text{O}-\text{C}$ ), carbonyl ( $\text{C}=\text{O}$ ), and carboxyl ( $\text{O}-\text{C}=\text{O}$ ).<sup>24,41,46,50</sup> Such functional groups interact with the groups of epoxy resin and form a strong mechanical interlocking at the fiber–matrix interface via a suitable bonding. Moreover, we use an amine-based hardener in order to solidify the fiber/epoxy network, which may form C–N bonds with GO coated fibers through a ring opening polymerization.<sup>18,45,51</sup> Therefore, the transverse tensile strength of GO-treated jute–fiber composites is higher than those of untreated fiber composites. In contrast, the coating with 1 and 10 mg/mL G flakes does not show a further noticeable improvement in the transverse tensile strength after the alkali treatment, which may be due to the absence of oxygen functional groups in the G flakes. Although a lower concentration ( $\sim 1$  mg/mL) of G flakes shows a slight improvement up to 6.5 MPa ( $\sim 23\%$  more) as compared to 10 mg/mL G flakes (only 4% improvement) and the HA0.5 treated fibers composite. The lower concentration of G flakes produce better mechanical interlocking on the fiber surface by diffusing into alkali-treated rough and porous structures of the jute fiber (Figure S5d, Supporting Information).<sup>6</sup> This results suggests that the GO modified jute fiber could significantly

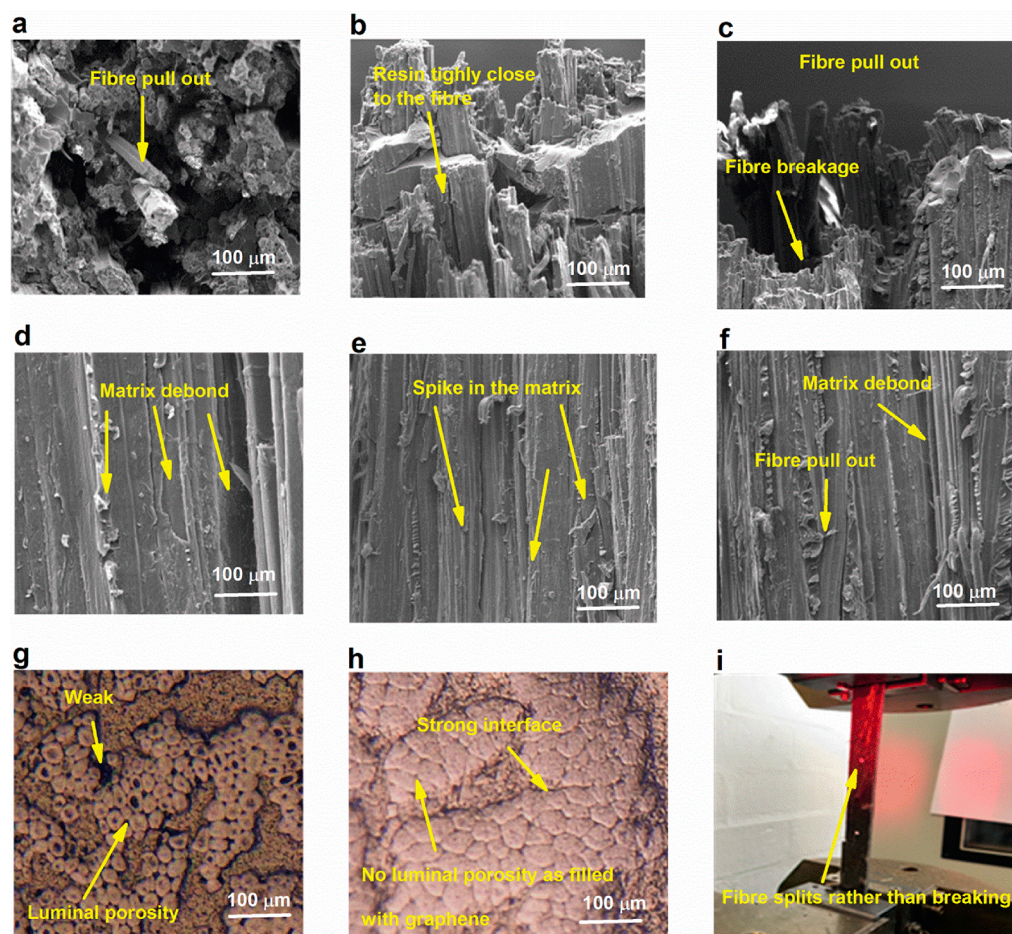


**Figure 4.** (a) Fracture surface of UT composites after the longitudinal tensile test ( $\times 250$ ); (b) fracture surface of GO 0.5-coated composites after the longitudinal tensile test ( $\times 250$ ); (c) fracture surface of G1 flake-modified composites after the longitudinal tensile test ( $\times 250$ ); (d) fracture surface of UT composites after the transverse tensile test ( $\times 250$ ); (e) fracture surface of GO 0.5-coated composites after the transverse tensile test ( $\times 250$ ); (f) fracture surface of G1 composites after the transverse tensile test ( $\times 250$ ); (g) optical microscopic cross-sectional image of alkali-treated jute fiber composites with higher magnification ( $\times 1000$ ); (h) optical microscopic cross-sectional image of GO-coated jute fiber composites with higher magnification ( $\times 1000$ ); and (i) fiber splits in the GO-coated specimen after the tensile test.

improve the interfacial adhesion between the jute fiber and epoxy matrix.

**Fracture Surface Topography.** We examined the fracture surface of the composites specimen after the longitudinal tensile test using a scanning electron microscope (SEM), Figure 4a–c. For the untreated jute fiber (Figure 4a), the surface of the composites fails predominantly by the weak interfacial bonding and the fiber pull-out. The uneven fiber breakage occurs along the direction of the fiber. With alkali-treated fibers, the rate of fiber pull-out reduces and even more fiber breakage is observed (Figure S8a, Supporting Information). This indicates an improvement in the interfacial bonding between the alkali treated jute fiber and epoxy matrix. Figure 4b shows a modified fracture surface for GO-coated jute fibers composites and strong bonding between resin and coated fibers. Moreover, the brittle appearance of the matrix (please see yellow arrow mark in Figure 4b) provides evidence of strong interfacial bonding that can lead to higher tensile properties of the composites. As discussed earlier, GO sheets introduced in the interfacial regions increase the strength and toughness at the interfacial regions due to the “crack healing” effect<sup>18</sup> and potential chemical bonding between the epoxy and GO sheets. As a result, the strong interface of GO-modified jute and the epoxy matrix transform the failure mode from the

fiber pull-out or debonding to the transverse fracture. Again, the G flake-modified jute fiber composites specimen shows more fiber debonding (Figure 4c) and pull-out. This may be due to the agglomeration of G flakes at the interfacial regions, which generates various types of stress concentration and thus reduces the strength at the interface.

We also examined the fracture surface of the transverse tensile test specimen by SEM in order to better understand the interfacial behavior and mechanical properties of the jute fiber–epoxy composites. The composite fracture section is shown in Figure 4d–f. Like a longitudinal specimen, the clean and smooth surfaces of the untreated jute fiber–epoxy reveals poor interfacial bonding of untreated jute fiber–epoxy composites. Figure 4d shows that the matrix is completely detached from the fiber (matrix debonding), due to the weak adhesion between the fiber and matrix. It indicates that the fiber matrix adhesion is the dominant mechanism of shear failure with the interface being the weakest part of the composites. The fracture surfaces of alkali-treated composites shows a grooved appearance in the image (Figure S8b, Supporting Information), which indicates the improvement of interface after alkali treatment of the jute fibers. However, there is still a matrix dominating debonding area in the fracture surface (Figure S8b, Supporting Information). Again for GO-modified jute fiber

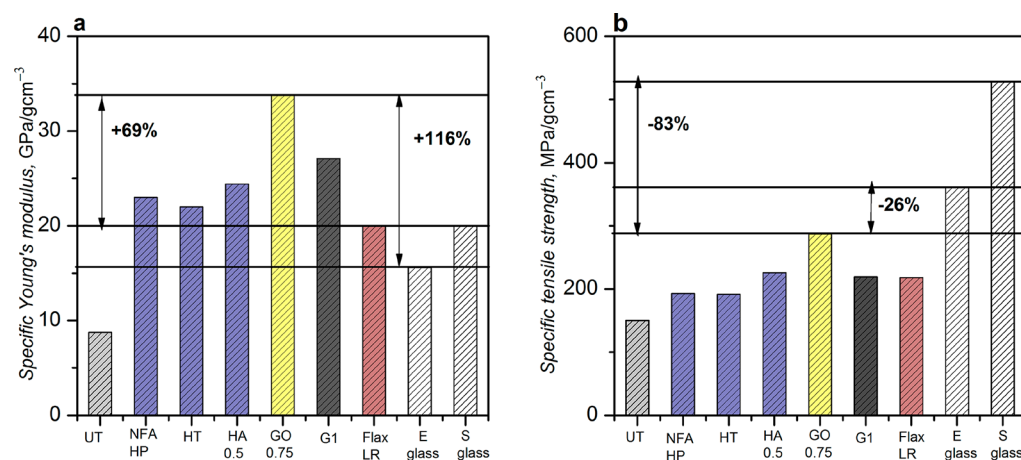


**Figure 5.** Comparative study of specific properties of untreated, new fiber architecture, alkali-treated, and graphene material-coated composites with Flax, E-glass, and S-glass fiber composites: (a) specific Young's modulus and (b) specific tensile strength (LR = data taken from the literature<sup>53</sup>).

**Table 1. Comparing Tensile Properties of Graphene-Coated Jute Fiber–Epoxy Composites with Other Natural Fibers in the Literature along with E and S-Glass Fiber–Epoxy Composites**

fibers	$V_f$ (%)	Young's modulus, GPa			tensile strength, MPa			ref
		before treatment	after treatment	change %	before treatment	after treatment	change %	
jute (NaOH 25%)	40	13.5	21.6	60	100	160	60	9
flax (NaOH 1%)	48b–53a <sup>a</sup>	23	25	8	282	283	0.35	53
kenaf (NaOH 6%)	48.6	10.34	10.7	3.5	95.4	106.3	11.5	40
sisal (NaOH 2%)	50	9.5	5	-47.3	275	320	16.3	43
carbon		45	55	22.2	1750	2000	14.28	54
jute (NaOH 0.5%)	54	27.6	32	16	232	282	21.5	this study
jute (GO 0.75%)	56	27.6	44.6	61.5	232	379	63.3	this study
E-glass	55		33.5			777		this study
S-glass	58		45			1187		this study

<sup>a</sup>b stands for before the test and a after the test.

composites, a significant change in the fracture surface are visible (Figure 4e), and we find a high amount of GO flakes sticking to the resin surface. Figure S5c shows the evidence of leaflike flakes on the fiber surface after the transverse tensile test, which creates small spikes on the resin surface (arrow mark in Figure 4e). This may be the outcome of strong interaction between the GO-modified jute fiber and the epoxy network and seems to be responsible for the improvement of interfacial shear strength of the composites. Figure 4f shows a deboned fracture surface of G flake-modified jute–epoxy composites and may be due to the lack of strong bonding between the G flakes and the jute fiber.

We then observed the cross section of alkali- and graphene-treated composites at higher magnification to study the porosity of the composites, Figure 4g,h. Figure 4g represents the interfacial porosity (luminal and impregnation porosity) present in alkali treated fiber composites. Such porosity may cause rapid failure of the composites in the transverse direction. Whereas in Figure 4h, such porosity is not visible as we introduce GO to alkali-treated jute fibers. We also examined the failed specimen of all samples after the longitudinal tensile test and find that all the samples fail catastrophically (Figure S7, Supporting Information) in the tensile test except GO 0.75-treated jute fiber composite specimens. Figure 4i shows fiber splitting in GO 0.75 composites during the failure of the composites, which

provides evidence of a strong interface of the composites and in agreement with tensile test results.

**Comparative Study.** We also made unidirectional E-glass and S-glass fiber reinforced epoxy composites in order to compare with our obtained results on jute fiber–epoxy composites. We then compare the obtained specific properties of untreated, new fiber architecture, alkali-treated, and graphene material-coated composites with Flax, E-glass, and S-glass fiber composites, Figure 5a,b. The specific Young's modulus of untreated jute fiber composites is found to be  $\sim 8.75$  GPa/g cm<sup>-3</sup>. Our newly developed jute fiber architecture increases the specific Young's modulus ( $\sim 23$  GPa/g cm<sup>-3</sup>) of composites significantly, which is higher than that of flax fibers, S-glass, and E-glass fiber composites. Please note we use the data from the literature for flax fiber composites with a higher volume fraction.<sup>53</sup> After coating jute fibers with GO, the Young's modulus of composites increases significantly to  $\sim 33.8$  GPa/g cm<sup>-3</sup> (Figure 5a), which is  $\sim 116\%$  and  $\sim 69\%$  higher than that of E ( $\sim 15.6$  GPa/g cm<sup>-3</sup>) and S ( $\sim 20$  GPa/g cm<sup>-3</sup>) glass fiber, respectively. Although the specific tensile strength of GO-coated composites is found to lower than that of S and E-glass fibers, the obtained specific tensile strength ( $\sim 287.29$  MPa/g cm<sup>-3</sup>) with GO-coated composites with NFA is found to be higher than any other natural fibers composites.

We then compare the tensile properties of jute fiber–epoxy composites of this study with other natural fiber-based epoxy

composites with a higher volume fraction reported in the literature, Table 1. A direct comparison is sometimes difficult as the experimental conditions in those studies are different. In addition, different fibers have different constituents' ratios, which have a direct impact on the mechanical properties. Table 1 shows a brief comparison between the results obtained in this study with results from previous studies obtained with various surface treatments on jute and other natural fiber-based composites. As found in the literature, traditional alkali treatment at lower concentration does not improve mechanical properties significantly. However, the jute fiber treated by GO and graphene flakes in our study shows a fairly a large increment in both the Young's modulus ( $\sim 61.5\%$  for GO) and tensile strength ( $\sim 63.3\%$  for GO) of the composites than the untreated one.

## CONCLUSION

In this work, we report on the individualization of jute fibers and nanoengineering with graphene oxides and graphene flakes in order to improve the mechanical properties of jute fiber–epoxy composites for high-performance natural composites applications. The individualization of jute fibers by combing improves the fiber packing of the composites significantly and results in a composite with new fiber architecture with higher mechanical performance. Further graphene coating on jute fibers promotes strong interfacial bonding and improved mechanical properties of the composites. Our nanoengineered graphene-based jute fiber composites provide higher mechanical performance and better specific properties than any other natural composites. The Young's modulus and tensile strength of jute–epoxy composites is increased by  $\sim 324\%$  and  $\sim 110\%$ , respectively, more than untreated jute fiber composites. The obtained specific modulus is also higher than that of glass, flax, and any other natural fiber composites, and specific tensile strength is comparable to that of E-glass. We believe our graphene-based jute fiber composites with NFA have potential to replace synthetic composites such as glass fibers for stiffness-driven structural applications.

## EXPERIMENTAL METHODS

**Materials.** The plant material (*Corchorus Olitorius*) known as "Tossa white jute" was obtained from Bangladesh, cultivated on the sandy loam plateau in the Northeast of Dhaka. The sample was cultivated from February to May in 2015. The annual rainfall of this area is  $\sim 500$ – $1500$  mm, and the temperature ranges from 20 to 33 °C. The content of long fibers in the bundles is  $\sim 98$ – $99$  wt %, whereas the rest 1–2 wt % is shives (cortical tissues and dust). The untreated long jute fiber has a golden color with an average length and diameter of  $\sim 2.9$  m and  $\sim 0.059$  mm, respectively. Analytical grade sodium hydroxide (NaOH) pellets (product no. 10502731) were purchased from Fisher Scientific, U.K. EL2 Epoxy Laminating Resin and AT30 Epoxy Hardener were purchased from Easy Composites, U.K. The natural flake graphite (average lateral size 50 mm) was kindly supplied by Graphexel Limited, U.K. Sodium deoxycholate (SDC) powder, potassium permanganate ( $\text{KMnO}_4$ ), sulfuric acid ( $\text{H}_2\text{SO}_4$ ,  $\sim 99\%$ ), and hydrogen peroxide ( $\text{H}_2\text{O}_2$ ,  $\sim 30\%$ ) were purchased from Sigma-Aldrich, U.K. S and E-glass fibers were purchased from AGY. EPI-REZ waterborne epoxy resin (product no. 7520-W-250) was purchased from Hexion, U.K. A modified Hummer's method that was described elsewhere was used to prepare graphene oxide (GO) in water.<sup>55</sup> Our previously reported method was followed to prepare microfluidized graphene flakes (G).<sup>28</sup> The lateral dimension of GO and G flakes are  $\sim 5.85$   $\mu\text{m}$  and  $\sim 4.86$   $\mu\text{m}$ , respectively, whereas the mean thickness of GO and G flakes are  $\sim 2.07$  nm and  $\sim 2.26$  nm, respectively.

**Alkali Treatment.** Untreated jute fibers were washed with deionized (DI) water after cutting into 30 cm long pieces, and they were then dried at 80 °C until a constant weight was achieved. These fibers were then treated in warm water at 60 °C for 60 min and then boiled at 100 °C for 30 min. The weight of fibers was reduced by  $\sim 6$  wt % and labeled as HT fibers. After these cleaning procedures, HT jute fibers were dipped in 0.5 wt % NaOH solutions with a 1:50 materials to liquor ratio (M/L) in order to remove hemicelluloses. The fibers obtained after two cycles of alkali treatment is termed as HA0.5 and loses almost a similar weight,  $\sim 6$  wt %, as reported in previous work.<sup>12</sup>

**Manufacturing of Graphene-Based Jute Fiber Preforms with NFA.** A unidirectional jute fiber matt was developed as a preform by combining physical and chemical treatments in three steps (Figure S1, Supporting Information). First, a hand-combing device was used to separate the elementary fiber from the technical fiber (Figure S1a, Supporting Information). The hand-comb was drawn along the length of the fiber at least twice to get a perfectly aligned and mostly individualized jute fiber, Figure S2b. Both edges of the perfectly aligned jute fiber preform was sealed using double-sided tape. Second, this preform was then coated with graphene materials (GO and G flakes) for 30 min with 1:10 M/L ratio and air-dried. The graphene materials coated jute fiber preform was then hand sprayed with 1 wt % EPI-REZ epoxy solution (binder). Finally, graphene-based preforms were hot pressed at 120 °C for 30 min at 1 Ton/inch<sup>2</sup> pressure and allowed to cool down to get 40 cm  $\times$  300 cm size preform with NFA, Figure S1f. A very small amount of binder ( $\sim 0.0015$  wt % EPI-REZ) was used in this study, which is epoxy (EL2) compatible with no significant effect on the properties of the resulting composites. We labeled the preforms as follows: untreated preform (UT), new fiber architecture preform after individualization (combing) (NFA), new fiber architecture preform with pressure (NFAWP), heat alkali treated preform (HA), graphene oxide-treated preform with 0.25, 0.50, 0.75, 1.0 mg/mL concentration were labeled as GO 0.25, GO 0.50, GO 0.75, and GO 1.0, respectively, and graphene flake-treated preform with 1 and 10 mg/mL concentrations were labeled as G 1.0 and G 10. Unidirectional glass fiber preforms were manufactured in order to compare its mechanical properties with that of jute fiber composites from this study (Figure S4a, Supporting Information).

**Composite Manufacturing by Vacuum Infusion Process.** A vacuum resin infusion process and room temperature thermoset EL2 epoxy resin was used to manufacture FRC. Briefly, four layers of UD jute preforms (dimensions 300 mm  $\times$  40 mm) are laid on a precleaned and precoated (with PVA release agent) metal plate. The sample was sealed by a plastic bag and vacuum pressed using a pump. EL2 Epoxy Laminating Resin and AT30 Epoxy Hardener were degassed separately for 30 min and mixed together immediately before we use. The resin with hardener then flowed over layered UD jute preforms at a constant flow rate using a vacuum pump, which enabled the impregnation of jute preforms with resin. The resin-infused preforms were then cured at room temperature for 24 h to make jute FRC for further characterization.

**Characterization.** An optical microscope (Keyence digital microscope VHX-500F, U.K.) was used to qualitatively measure the image of fiber packing arrangement of the composites (Figure S2, Supporting Information) and flake size of graphene materials. A Philip XL-30 field emission gun scanning electron microscope (SEM) was used to analyze the surface topography of fractured jute fiber composites. The surface characteristics of graphene materials was analyzed using a Kratos axis X-ray photoelectron spectroscopy (XPS) system. A Dimension Icon (Bruker) atomic force microscope (AFM) was used to determine the flake thickness. A Renishaw Raman system equipped with a 633 nm laser was used to collect Raman spectra of the graphene flakes.

**Volume Fraction and Density.** The fiber volume fraction of laminates was calculated using the ratio of the mass of the preformed  $W_f$  and the resulting laminate  $W_c$ . The composite density  $\rho_c$  was measured using the specimen chamber temperature of  $20 \pm 1$  °C.



The fiber volume fraction  $V_f$ , matrix volume fraction  $V_m$ , and void volume fraction  $V_p$  of the composites were calculated using eq 1, where  $w$  and  $\rho$  are the weight and density, respectively, while the subscripts f, m, and c denote fibers, matrix, and composite, respectively.

$$V_f = \frac{\rho_c}{\rho_f} w_f; \quad V_m = \frac{\rho_c}{\rho_m} (1 - w_f); \quad V_p = \frac{(\rho_{th} - \rho_{exp})}{\rho_{th}} \quad (1)$$

Density measurements were carried out according to ASTM-D3800-99 in an AJ50L (Mettler Toledo, U.K.) analytical balance. We weighed the untreated and treated composites in the air and then in water. The weight difference between the two media is called the buoyance force.<sup>36</sup> We calculate the density of the composites by using the following formula (eq 2).

$$\rho_c = \frac{M_1}{(M_1 - M_2)} (\rho_1 - \rho_{air}) + \rho_{air} \quad (2)$$

where  $\rho_1$  is the density of paper oil,  $\rho_{air}$  is the density of air,  $M_1$  is the weight of sample in air, and  $M_2$  is the weight of sample in liquid, respectively. For each laminate, a minimum of five samples were tested and the average of five samples was calculated as the final density of the composites.

**Mechanical Testing of the Composites.** The longitudinal tensile test was carried out to determine the tensile properties (Young's modulus and tensile strength) of the unidirectional jute fiber composites. The test was conducted as per ASTM D3039 standard using an Instron 5985 (U.K.) testing machine equipped with a 100 kN load cell and a video extensometer (Figure S6). Five 250 mm long and 15 mm wide specimens were tested for each type of composite at a cross-head speed of 2 mm/min. The Young's modulus, tensile strength, and tensile failure strain were measured from the obtained stress-strain curve. In addition, a transverse tensile test was carried out to understand the effect of GO and G flakes on the mechanical properties of the composites.

## ■ ASSOCIATED CONTENT

### 📄 Supporting Information

The Supporting Information is available free of charge on the ACS Publications website at DOI: 10.1021/acsami.9b04696.

Design, manufacturing of jute fiber preform and its composites; preparation of jute and glass fiber preform; single fiber properties; microscopy and density of the composites; tensile test and mechanical properties of the composites; and optical and SEM images of the fracture surface of jute-epoxy composites with untreated, treated, and coated samples (PDF)

## ■ AUTHOR INFORMATION

### Corresponding Authors

\*E-mail: mdnazmul.karim@manchester.ac.uk.

\*E-mail: prasad.potluri@manchester.ac.uk.

### ORCID

Nazmul Karim: 0000-0002-4426-8995

### Author Contributions

N.K. conceived the idea of graphene-based natural jute fibre composites, and together with F.S., N.K. designed the experiments. F.S. prepared the samples, performed the measurements, and carried out data analysis under supervision of N.K. and P.P. N.K. wrote the manuscript with input from F.S. and K.S.N. S.A. prepared, characterized, and analyzed the graphene materials.

### Notes

The authors declare no competing financial interest.

## ■ ACKNOWLEDGMENTS

This work was supported by EU Graphene Flagship Program, European Research Council Synergy Grant Hetero2D, the Royal Society, and Engineering and Physical Sciences Research Council, U.K. (EPSRC Grant Number EP/N010345/1, 2015). The authors kindly acknowledge the Commonwealth Scholarship Commission, U.K. and the Government of Bangladesh for the Ph.D. funding of Forkan Sarker and Shaila Afroj, respectively.

## ■ REFERENCES

- Pickering, K. L.; Efendy, M. G. A.; Le, T. M. A Review of Recent Developments in Natural Fibre Composites and Their Mechanical Performance. *Composites, Part A* **2016**, *83*, 98–112.
- Karim, M. N.; Afroj, S.; Rigout, M.; Yeates, S. G.; Carr, C. Towards UV-Curable Inkjet Printing of Biodegradable Poly (Lactic Acid) Fabrics. *J. Mater. Sci.* **2015**, *50*, 4576–4585.
- Potluri, P.; Perez Ciurezu, D. A.; Ramgulum, R. B. Measurement of Meso-Scale Shear Deformations For Modelling Textile Composites. *Composites, Part A* **2006**, *37*, 303–314.
- Sepe, R.; Bollino, F.; Boccardo, L.; Caputo, F. Influence of Chemical Treatments on Mechanical Properties of Hemp Fiber Reinforced Composites. *Composites, Part B* **2018**, *133*, 210–217.
- Faruk, O.; Sain, M. *Biofiber Reinforcements in Composite Materials*; Elsevier, 2014.
- Sarker, F.; Karim, N.; Afroj, S.; Koncherry, V.; Novoselov, K. S.; Potluri, P. High-Performance Graphene-Based Natural Fiber Composites. *ACS Appl. Mater. Interfaces* **2018**, *10*, 34502–34512.
- Chen, J.; Zhao, D.; Jin, X.; Wang, C.; Wang, D.; Ge, H. Modifying Glass Fibers with Graphene Oxide: Towards High-Performance Polymer Composites. *Compos. Sci. Technol.* **2014**, *97*, 41–45.
- Tzounis, L.; Debnath, S.; Roop, S.; Fischer, D.; Mäder, E.; Das, A.; Stamm, M.; Heinrich, G. High Performance Natural Rubber Composites with a Hierarchical Reinforcement Structure of Carbon Nanotube Modified Natural Fibers. *Mater. Eng.* **2014**, *58*, 1–11.
- Gassan, J.; Bledzki, A. K. Alkali Treatment of Jute Fibers: Relationship Between Structure And Mechanical Properties. *J. Appl. Polym. Sci.* **1999**, *71*, 623–629.
- Roy, M. Mechanical Properties of Jute II: The Study of Chemically Treated Fibres. *J. Text. I. Trans.* **1953**, *44*, T44–T52.
- Bachtar, D.; Sapuan, S.; Hamdan, M. The Effect of Alkaline Treatment on Tensile Properties of Sugar Palm Fibre Reinforced Epoxy Composites. *Mater. Eng.* **2008**, *29*, 1285–1290.
- Roy, A.; Chakraborty, S.; Kundu, S. P.; Basak, R. K.; Majumder, S. B.; Adhikari, B. Improvement in Mechanical Properties of Jute Fibres Through Mild Alkali Treatment as Demonstrated by Utilisation of the Weibull Distribution Model. *Bioresour. Technol.* **2012**, *107*, 222–228.
- Saha, P.; Manna, S.; Chowdhury, S. R.; Sen, R.; Roy, D.; Adhikari, B. Enhancement of Tensile Strength of Lignocellulosic Jute Fibers by Alkali-Steam Treatment. *Bioresour. Technol.* **2010**, *101*, 3182–3187.
- Chen, L.; Wei, F.; Liu, L.; Cheng, W.; Hu, Z.; Wu, G.; Du, Y.; Zhang, C.; Huang, Y. Grafting of Silane and Graphene Oxide onto PBO Fibers: Multifunctional Interphase for Fiber/Polymer Matrix Composites with Simultaneously Improved Interfacial and Atomic Oxygen Resistant Properties. *Compos. Sci. Technol.* **2015**, *106*, 32–38.
- Du, S.-S.; Li, F.; Xiao, H. M.; Li, Y. Q.; Hu, N.; Fu, S. Y. Tensile and Flexural Properties of Graphene Oxide Coated-Short Glass Fiber Reinforced Polyethersulfone Composites. *Composites, Part B* **2016**, *99*, 407–415.
- Pathak, A. K.; Borah, M.; Gupta, A.; Yokozeki, T.; Dhakate, S. R. Improved Mechanical Properties of Carbon Fiber/Graphene Oxide-Epoxy Hybrid Composites. *Compos. Sci. Technol.* **2016**, *135*, 28–38.

- (17) Tang, L. C.; Wan, Y. J.; Yan, D.; Pei, Y. B.; Zhao, L.; Li, Y. B.; Wu, L. B.; Jiang, J. X.; Lai, G. Q. The effect of Graphene Dispersion on the Mechanical Properties of Graphene/Epoxy Composites. *Carbon* **2013**, *60*, 16–27.
- (18) Zhang, X.; Fan, X.; Yan, C.; Li, H.; Zhu, Y.; Li, X.; Yu, L. Interfacial Microstructure and Properties of Carbon Fiber Composites Modified with Graphene Oxide. *ACS Appl. Mater. Interfaces* **2012**, *4*, 1543–1552.
- (19) Doan, T.-T.-L.; Brodowsky, H.; Mäder, E. Jute Fibre/Epoxy Composites: Surface Properties And Interfacial Adhesion. *Compos. Sci. Technol.* **2012**, *72*, 1160–1166.
- (20) Hill, C. A.; Khalil, H. A.; Hale, M. D. A Study of the Potential of Acetylation to Improve the Properties of Plant Fibres. *Ind. Crops Prod.* **1998**, *8*, 53–63.
- (21) Papadopoulos, A. Chemical Modification of Solid Wood and Wood Raw Material for Composites Production with Linear Chain Carboxylic Acid Anhydrides: A Brief Review. *Bioresources* **2010**, *5* (1), 1–8.
- (22) Sreekala, M.; Kumaran, M.; Thomas, S. Water Sorption in Oil Palm Fiber Reinforced Phenol Formaldehyde Composites. *Composites, Part A* **2002**, *33*, 763–777.
- (23) Seki, Y.; Sarikanat, M.; Sever, K.; Erden, S.; Gulec, H. A. Effect of the Low and Radio Frequency Oxygen Plasma Treatment of Jute Fiber on Mechanical Properties of Jute Fiber/Polyester Composite. *Fibers Polym.* **2010**, *11*, 1159–1164.
- (24) Afroj, S.; Karim, N.; Wang, Z.; Tan, S.; He, P.; Holwill, M.; Ghazaryan, D.; Fernando, A.; Novoselov, K. S. Engineering Graphene Flakes for Wearable Textile Sensors via Highly Scalable and Ultrafast Yarn Dyeing Technique. *ACS Nano* **2019**, *13*, 3847.
- (25) He, P.; Brent, J. R.; Ding, H.; Yang, J.; Lewis, D. J.; O'Brien, P.; Derby, B. Fully Printed High Performance Humidity Sensors Based on Two-Dimensional Materials. *Nanoscale* **2018**, *10*, 5599–5606.
- (26) Ma, P. C.; Liu, J. W.; Gao, S. L.; Mäder, E. Development of Functional Glass Fibres with Nanocomposite Coating: A Comparative Study. *Composites, Part A* **2013**, *44*, 16–22.
- (27) Wan, Y. J.; Tang, L. C.; Gong, L. X.; Yan, D.; Li, Y. B.; Wu, L. B.; Jiang, J. X.; Lai, G. Q. Grafting of Epoxy Chains onto Graphene Oxide for Epoxy Composites with Improved Mechanical and Thermal Properties. *Carbon* **2014**, *69*, 467–480.
- (28) Karim, N.; Zhang, M.; Afroj, S.; Koncherry, V.; Potluri, P.; Novoselov, K. S. Graphene-Based Surface Heater for De-Icing Applications. *RSC Adv.* **2018**, *8*, 16815–16823.
- (29) Idumah, C. I.; Hassan, A. Hibiscus Cannabinus Fiber/PP Based Nano-Biocomposites Reinforced with Graphene Nanoplatelets. *J. Nat. Fibers* **2017**, *14*, 691–706.
- (30) Qin, W.; Vautard, F.; Drzal, L. T.; Yu, J. Mechanical and Electrical Properties of Carbon Fiber Composites with Incorporation of Graphene Nanoplatelets at the Fiber–Matrix Interphase. *Composites, Part B* **2015**, *69*, 335–341.
- (31) Yavari, F.; Rafiee, M.; Rafiee, J.; Yu, Z.-Z.; Koratkar, N. Dramatic Increase in Fatigue Life in Hierarchical Graphene Composites. *ACS Appl. Mater. Interfaces* **2010**, *2*, 2738–2743.
- (32) Li, S.; Li, Z.; Burnett, T. L.; Slater, T. J. A.; Hashimoto, T.; Young, R. J. Nanocomposites of Graphene Nanoplatelets in Natural Rubber: Microstructure and Mechanisms of Reinforcement. *J. Mater. Sci.* **2017**, *52*, 9558–9572.
- (33) Yang, Y.; Hou, H.; Zou, G.; Shi, W.; Shuai, H.; Li, J.; Ji, X. Electrochemical Exfoliation of Graphene-Like Two-Dimensional Nanomaterials. *Nanoscale* **2019**, *11*, 16–33.
- (34) Ashby, M. F.; Jones, D. R. H. *Engineering Materials 1: An Introduction to Properties, Applications and Design*; Elsevier, 2012; Vol. 1.
- (35) Hughes, M.; Carpenter, J.; Hill, C. Deformation and Fracture Behaviour of Flax Fibre Reinforced Thermosetting Polymer Matrix Composites. *J. Mater. Sci.* **2007**, *42*, 2499–2511.
- (36) Larco, C.; Pahonie, R.; Edu, I. The Effects of Fibre Volume Fraction on a Glass-Epoxy Composite Material. *INCAS Bulletin* **2015**, *7*, 113.
- (37) Madsen, B.; Thygesen, A.; Lilholt, H. Plant Fibre Composites—Porosity and Stiffness. *Compos. Sci. Technol.* **2009**, *69*, 1057–1069.
- (38) Shah, D. U.; Schubel, P. J.; Clifford, M. J.; Licence, P. Mechanical Property Characterization of Aligned Plant Yarn Reinforced Thermoset Matrix Composites Manufactured via Vacuum Infusion. *Polym.-Plast. Technol. Eng.* **2014**, *53*, 239–253.
- (39) Madsen, B.; Lilholt, H. Physical and Mechanical Properties of Unidirectional Plant Fibre Composites—An Evaluation of the Influence of Porosity. *Compos. Sci. Technol.* **2003**, *63*, 1265–1272.
- (40) Fiore, V.; Di Bella, G.; Valenza, A. The effect of Alkaline Treatment on Mechanical Properties of Kenaf Fibers and Their Epoxy Composites. *Composites, Part B* **2015**, *68*, 14–21.
- (41) Abdelkader, A. M.; Karim, N.; Vallés, C.; Afroj, S.; Novoselov, K. S.; Yeates, S. G. Ultraflexible and Robust Graphene Supercapacitors Printed on Textiles for Wearable Electronics Applications. *2D Mater.* **2017**, *4*, No. 035016.
- (42) Bos, H.; Van Den Oever, M.; Peters, O. Tensile and Compressive Properties of Flax Fibres for Natural Fibre Reinforced Composites. *J. Mater. Sci.* **2002**, *37*, 1683–1692.
- (43) Kalyanasundaram, S.; Jayabal, S. The Effect of Fiber Treatment on the Mechanical Properties of Christmas Palm Fiber-Polyester Composites. *Appl. Mech. Mater.* **2013**, *467*, 208–214.
- (44) Agarwal, B. D.; Broutman, L. J.; Chandrashekhara, K. *Analysis and Performance of Fiber Composites*; John Wiley & Sons, 2017.
- (45) Wang, H.; Xian, G.; Li, H. Grafting of Nano-TiO<sub>2</sub> onto Flax Fibers and the Enhancement of the Mechanical Properties of the Flax Fiber and Flax Fiber/Epoxy Composite. *Composites, Part A* **2015**, *76*, 172–180.
- (46) Karim, N.; Afroj, S.; Tan, S.; He, P.; Fernando, A.; Carr, C.; Novoselov, K. S. Scalable Production of Graphene-Based Wearable E-textiles. *ACS Nano* **2017**, *11*, 12266–12275.
- (47) Xiong, R.; Grant, A. M.; Ma, R.; Zhang, S.; Tsukruk, V. V. Naturally-Derived Biopolymer Nanocomposites: Interfacial Design, Properties and Emerging Applications. *Mater. Sci. Eng., R* **2018**, *125*, 1–41.
- (48) Karim, N.; Afroj, S.; Tan, S.; Novoselov, K. S.; Yeates, S. G. All Inkjet-Printed Graphene-Silver Composite Ink on Textiles for Highly Conductive Wearable Electronics Applications. *Sci. Rep.* **2019**, *9* (1), 8035.
- (49) Xiong, R.; Kim, H. S.; Zhang, L.; Korolovych, V. F.; Zhang, S.; Yingling, Y. G.; Tsukruk, V. V. Wrapping Nanocellulose Nets around Graphene Oxide Sheets. *Angew. Chem., Int. Ed.* **2018**, *57*, 8508–8513.
- (50) Karim, N.; Afroj, S.; Malandraki, A.; Butterworth, S.; Beach, C.; Rigout, M.; Novoselov, K. S.; Casson, A. J.; Yeates, S. G. All Inkjet-Printed Graphene-Based Conductive Patterns for Wearable E-Textile Applications. *J. Mater. Chem. C* **2017**, *5*, 11640–11648.
- (51) Yang, H.; Shan, C.; Li, F.; Zhang, Q.; Han, D.; Niu, L. Convenient Preparation of Tunably Loaded Chemically Converted Graphene Oxide/Epoxy Resin Nanocomposites from Graphene Oxide Sheets Through Two-Phase Extraction. *J. Mater. Chem.* **2009**, *19*, 8856–8860.
- (52) Herrera-Franco, P.; Valadez-Gonzalez, A. Mechanical Properties of Continuous Natural Fibre-Reinforced Polymer Composites. *Composites, Part A* **2004**, *35*, 339–345.
- (53) Van de Weyenberg, I.; Truong, T. C.; Vangrimde, B.; Verpoest, I. Improving the Properties of UD Flax Fibre Reinforced Composites by Applying An Alkaline Fibre Treatment. *Composites, Part A* **2006**, *37*, 1368–1376.
- (54) Zhang, R. L.; Gao, B.; Ma, Q. H.; Zhang, J.; Cui, H. Z.; Liu, L. Directly Grafting Graphene Oxide onto Carbon Fiber and the Effect On the Mechanical Properties of Carbon Fiber Composites. *Mater. Des.* **2016**, *93*, 364–369.
- (55) Hummers, W. S., Jr; Offeman, R. E. Preparation of Graphitic Oxide. *J. Am. Chem. Soc.* **1958**, *80*, 1339–1339.
- (56) Orue, A.; Jauregi, A.; Unsuain, U.; Labidi, J.; Eceiza, A.; Arbelaz, A. The Effect of Alkaline and Silane Treatments on Mechanical Properties and Breakage of Sisal Fibers and Poly (Lactic Acid)/Sisal Fiber Composites. *Composites, Part A* **2016**, *84*, 186–195.

**■ NOTE ADDED AFTER ASAP PUBLICATION**

This paper was published on the Web on May 30, 2019, with references 47 and 48 duplicated. Reference 47 was corrected and the Table of Contents/Abstract graphic was replaced due to a slight error in the arrow position, and the corrected version was reposted on May 31, 2019.